厚生労働科学研究費補助金
医療機器開発推進研究事業

極細径内視鏡用高機能中空ファイバの製作に関する研究

平成20年度　総括研究報告書

研究代表者　岩井　克全

平成21（2009）年3月

厚生労働科学研究費補助金
医療機器開発推進研究事業

極細径内視鏡用高機能中空ファイバの製作に関する研究

平成20年度　総括研究報告書

研究代表者　岩井　克全

平成21（2009）年3月

目　　次

厚生労働科学研究費補助金（医療機器開発推進研究事業）
（総括）研究報告書

極細径内視鏡用高機能中空ファイバの製作に関する研究

研究代表者　岩井　克全　仙台電波工業高等専門学校情報通信工学科　助教

研究要旨：本研究では、①無機材料が内面にコートされた銀中空ファイバを用いる、②内径 0.1 mm の細径中空ファイバ、③製作法が単純、低コスト化が可能の特長を有する超細径中空ファイバの製作を目的とする。高エネルギー伝送ならびに滅菌工程に耐える超細径中空ファイバが実現できれば、歯科内視鏡などの低侵襲治療の高効率化を図ることが可能である。

研究分担者
なし

A．研究目的

治療用の数多くのレーザの中、波長が 2 μm 以上の赤外波はその有効性が確認されつつも、レーザ発振器から患部へのレーザ光の導光手段は従来の石英光ファイバが使えないため、最近は図 1 のような中空ファイバが多く使用されてきている。

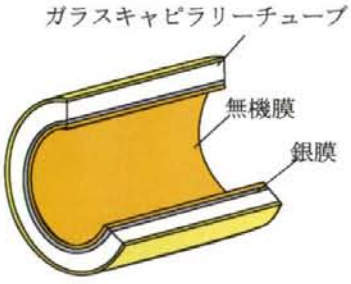

図 1 中空ファイバの構造

中空ファイバで効率的な内視鏡治療を行うためには、患部に接触して使用できること、高効率でレーザ光を導光できること、高エネルギー伝送に耐えること、内視鏡に挿入可能な細径ファイバであることが要求されている。現時点ではこの要求性能を満たす中空ファイバが無いため、導光効率を犠牲にした短尺の中実のガラスファイバ素子が使用されている。極細径内視鏡用の場合、ファイバの細径化によるレーザエネルギー密度の増加で従来の光学ポリマー膜の損傷が問題となるが、最近、耐久性に極めて優れた無機ガラス材料を用いた中空ファイバ（内径 0.7 mm、長さ 10 cm)の試作に成功した。無機ガラス薄膜を内装した超細径中空ファイバが実現されれば、その導光効率の高さ、高耐久性のメリットで、歯科内視鏡(図 2, 3 参照)などの低侵襲治療の高効率化を図ることが可能である。

図 2 歯科内視鏡

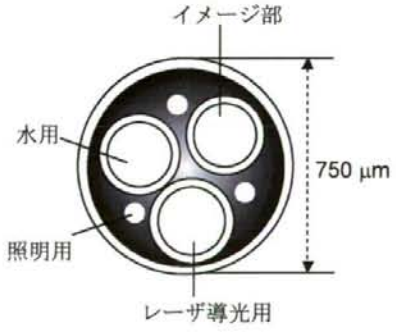

図 3 内視鏡の先端部

本研究では、図 4 のように使用可能な超細径中空ファイバとして、

①無機材料が内面にコートされた銀中空ファイバを用いる

②外径 0.17 mm、内径 0.1 mm の細径中空ファイバとして機能する

③製作法が単純で、低コスト化が可能であるの特長を有し、現存する赤外伝送路に対して、機能、価格の上で極めて優位に立つことが期待される超細径中空ファイバの製作を目的とする。

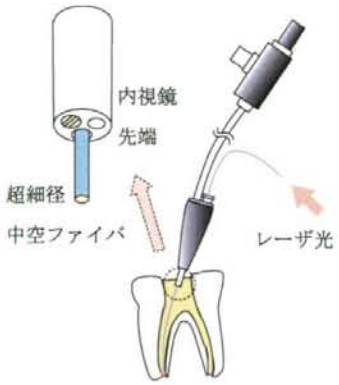

図 4 内視鏡用中空ファイバ

達成すべき課題の事業年度並びに数値レベルは、以下の通りである。

①平成 20 年度　超細径銀中空ファイバの製作
　内径 0.1 mm、長さ 25cm
②平成 21 年度　無機ガラス薄膜内装中空ファイバの製作
　内径 0.1 mm、長さ 10cm、Er:YAG 透過率 60%
③平成 22 年度　超細径中空ファイバの先端封止技術の開発
　先端封止部の Er:YAG 透過率 70%

なお、現状では、レーザ光用の先端装置で、赤外光の透過率は 30 %を越えるものはない。このことはレーザへの要求を半減できる。また、本研究で提案するような細径中空ファイバは存在しない。

技術課題は、中空ファイバの銀膜の成膜が本質的な課題であり、内径 0.1 mm、長さ 25 c mの超細径銀中空ファイバの製作を目標とする。

B．研究方法

赤外レーザ光を低損失かつフレキシブルに伝送可能な伝送路として、ガラスキャピラリチューブ内面に銀層と光学膜を形成した光学膜内装銀中空ファイバがある。中空ファイバの伝送損失を増大させる原因は銀層の表面粗さである。粗さが大きいために、可視波長帯において散乱損失が大きくなり、また均一な光学膜の形成も困難になる。低損失な中空ファイバを実現するためにはできる限り平滑な銀層を形成することが必要となる。銀中空ファイバの製作は極めて内面が整い、構造不整小さなガラスキャピラリチューブの内面に銀鏡反応により銀を無電解析出させて行う。銀鏡反応法とは、硝酸銀溶液を還元剤で金属に還元し、目的の基板上に銀の膜として付着させる方法である。無電解析出させた銀層と基板ガラスとの境界面には粗さの極めて小さく光沢のある銀面が容易に製作できる。銀鏡反応の前処理として $SnCl_2$ 溶液を用いることにより、付着面が活性化され、銀膜の成膜速度が向上することが知られている。これまでにも中空ファイバ製作において $SnCl_2$ 溶液の前処理を行い、銀層を形成する例が示されており、内径 0.1 mm 銀中空ファイバの製作においても $SnCl_2$ 溶液を用いる。

また銀鏡反応の際、中空ファイバの内径が細いと流量は減り、図 5 のようにガラスキャピラリチューブ中を流れる間に銀粒子が大きくなり、ファイバ内面に粗い銀が形成される。

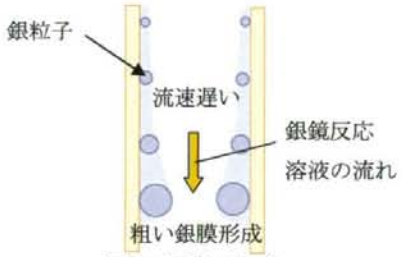

図 5 銀膜の形成

内径 0.7 mm 銀中空ファイバ製作においては、図 6 左図に示すような銀鏡装置でガラスキャピラリチューブを単一で並列接続しただけで低損失なファイバを製作できたが、超細径中空ファイバで

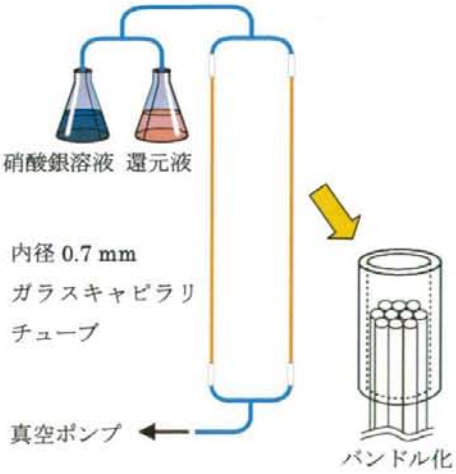

図 6 銀中空ファイバの製作装置

は溶液が流れず、銀を成膜することはできない。そこで図 6 右図のように、ガラスキャピラリチューブ (内径 0.1 mm、長さ 50 cm)を束ねたバンドルを製作し、流量の増加を行う。流量は、内径 0.7 mm 銀中空ファイバの製作条件から 15 ml/min 程度を目標とする。

内径 3 mm のシリコーンチューブ内にガラスキャピラリチューブ(内径 0.1 mm、長さ 50 cm)280 本を入れ、エポキシ樹脂により接着して、バンドル束を製作した。蒸留水を用いてバンドル束の流量の測定を行った結果を図 7 に示す。

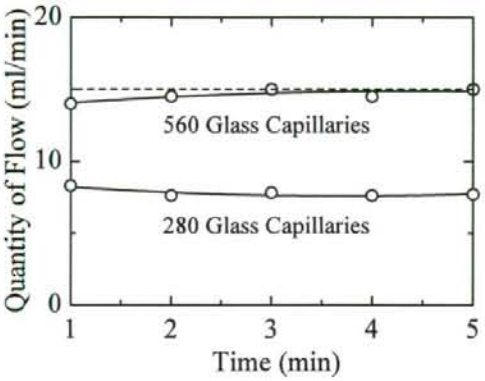

図 7　ガラスキャピラリチューブの本数に対する流量

560 本のバンドル束ではチューブ断面が大きく、銀鏡反応溶液が均等に流れないため、銀中空ファイバの伝送特性にばらつきが大きく生じると思われる。内径 0.1 mm のガラスキャピラリチューブ 280 本束を 2 個製作し並列に接続して流量は 14.5 ml/min となり、ほぼ目標の流量を実現することができた。

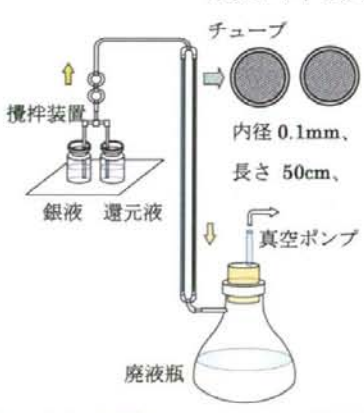

図 8 超細径銀中空ファイバの製作装置

図 8 に、上記のバンドル束 2 個を用いて構築した内径 0.1 mm 超細径中空ファイバの銀膜形成装置を示す。銀鏡条件は、

① 前処理液に $SnCl_2$ 溶液を用いる
② 銀鏡溶液温度は 18 度
③ 銀鏡時間は 3 分

である。銀鏡溶液温度は、高いほど銀粒子の成長は早くなる傾向があるため、銀粒子の成長を抑えるために低温の 18 度とした。$SnCl_2$ 溶液を用いる前処理により、従来法に比べ、ガラスキャピラリチューブに銀が付着する速度が飛躍的に速くなり、短時間で銀膜形成が可能になった。銀鏡時間は、これまでに製作した内径 0.7 mm の銀中空ファイバの製作条件から、銀鏡時間 3 分を用いた。

銀鏡反応後、窒素雰囲気(流量 300 ml/min)で 150℃の加熱乾燥工程を 30 分行った。

(倫理面への配慮)

当該研究は、倫理面の問題がない。生命倫理・安全対策に対する取り組みが必要とされている研究に該当しない。

C．研究結果・考察

光スペクトラムアナライザを用いて、銀中空ファイバ(内径 0.1 mm、長さ 35 cm)の損失波長スペクトルの測定を行った。図 9 に超細径銀中空ファイバ(10 本)の波長損失特性を示す。

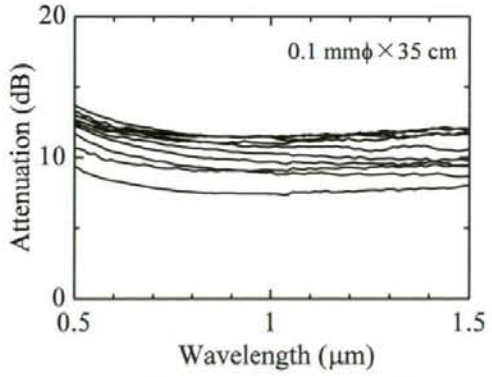

図 9 超細径銀中空ファイバの波長損失特性
但し、内径 0.1mm、長さ 35 cm 銀中空ファイバ使用、FWHM10.6° のガウスビームで励振されている。

損失の最大値と最小値の差が 4.1 dB 程度とファイバの伝送特性にばらつきがあることが分った。バンドル形成の際、端面を揃える事が難しく、溶液の流れ易さがファイバで異なったためと思われ

る。波長 1 μm において、最も低損失なファイバ(長さ 35 cm)は 7.5 dB であり、低損失なファイバを製作できることが分った。銀膜の粗さが大きい場合、波長 1 μm よりも短波長で損失は大きく増加する。製作した銀中空ファイバは波長 0.7 μm 程度まで損失が低く、短波長域での散乱損失が抑えられており、粗さの小さい銀を形成することに成功したと思われる。またバンドル化のより、1 回の銀鏡反応工程で、560 本の銀中空ファイバを製作することが出来る。

280 本束の外側のファイバと内側のファイバを 5 本ずつ切り出し、可視～近赤外波長帯の損失波長スペクトル (FWHM10.6 ° のガウスビームで励振)の測定を行った。図 10 に超細径銀中空ファイバの波長損失特性を示す。図中に、束の外側の銀中空ファイバの測定値の最小と最大損失のものを破線で示し、内側の銀中空ファイバの最小と最大損失のものを実線で示す。どちらも最大損失と最小損失値にばらつきが生じている。原因は、バンドルの製作の際に、ファイバ端面を揃えるのが難しく、溶液の流量が各ファイバで異なったためと思われる。束の外側の銀中空ファイバより、内側の銀中空ファイバの方が、損失値が低い傾向があり、これは外側のファイバは、シリコーンチューブとの間に隙間ができ、ガラスキャピラリチューブ内を流れる銀鏡反応溶液の流量が安定していなかったためと思われる。

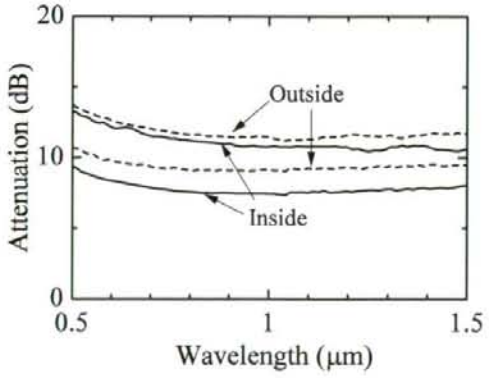

図 10 超細径銀中空ファイバの波長損失特性
但し、内径 0.1mm、長さ 35 cm 銀中空ファイバ使用、FWHM10.6° のガウスビームで励振されている。

次に、従来の各種内径 (0.25 mm～1 mm)銀中空ファイバと内径 0.1 mm 銀中空ファイバの伝送損失を比較するために、可視～近赤外波長帯の損失波長スペクトル (FWHM10.6 ° のガウスビームで励振)の測定を行った。測定法としては、カットバック法を用いる。この方法は被測定中空ファイバを切断するため、ファイバ長は短くなるが、測定系の入射部・受光部における接続損失を含まないため伝送損失を厳密に測定できる。まず、リファレンスファイバとして長さ 10 cm の銀中空ファイバの測定を行い、次に 30 cm の銀中空ファイバの伝送損失を測定し、その値から、長さ 20 cm の中空ファイバの伝送損失を求めた。各種内径中空ファイバの波長損失特性を図 11 に示す。

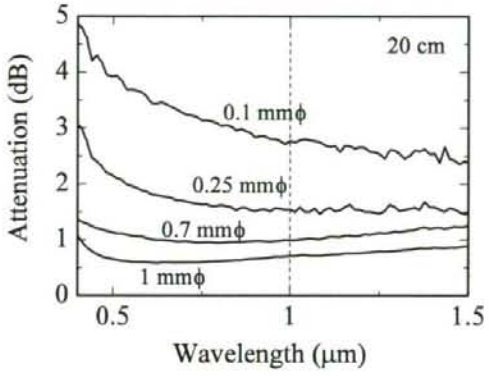

図 11 各種内径の中空ファイバ(長さ 20 cm)に対する波長損失特性
但し、FWHM10.6 °のガウスビームで励振

図 9 の損失値より、波長 1 μm において 3 dB 程度と低損失になっている。これは、測定系の接続損失が含まれないためと思われる。

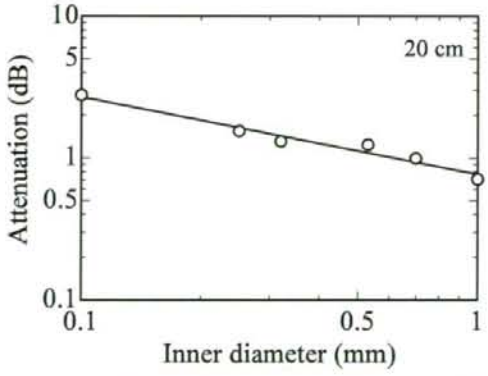

図 12 各種内径の中空ファイバ(長さ 20 cm)に対する伝送損失
但し、波長 1 μm の損失値
FWHM10.6 °のガウスビームで励振

次に各種内径中空ファイバの波長 1 μm における伝送損失値を図 12 に示す。中空ファイバの伝送損失は、理論的にはファイバ内径の 3 乗に逆比例する。各種内径 (内径 1 mm～0.25 mm)の銀中空ファイバの伝送損失値と比較した結果、内径 0.1 mm 銀中空ファイバの損失値は、各種内径の損失値付近を通る直線とほぼ一致することから、ファイバ内面に良好な銀膜の形成に成功したと思われる。

D．結論

従来の導光効率を犠牲にした Er:YAG レーザ用の短尺な充実型ガラスファイバに対して、高エネルギー伝送ならびに滅菌工程に耐える超細径中空ファイバが実現できれば、内視鏡治療において、Er:YAG レーザ光を効率よく用いることができる。また導光効率の飛躍的な向上により、レーザ光源の低出力化に繋がり経済性のメリットも生じる。現在、用いられている医療用レーザ装置の短尺な充実型ガラスファイバは、加工工程が複雑なため高価である。一方中空ファイバは簡単な構造で安価に製造でき、消耗品のコストを下げることができるため、医療費の抑制に繋がる。最小侵襲治療が叫ばれている医療現場において、レーザによる低侵襲治療は社会的な要求であり、それに関連する治療装置の開発は極めてニーズが大きい。経済性を考慮しつつ、医療現場において感染症を防止することも重要な課題である。これらの要求を一度に満たす手段として、耐久性の高い無機材料を用い、製作が容易でしかも滅菌可能な、もしくはディスポーザブルな医療用ファイバを実現することは、極めて大きな意味を持つ。また、治療・療養期間の短縮化、高齢者保護の上で、その社会的な効果も十分ある。平成 20 年度に超細径銀中空ファイバの製作の製作を行い、
目標値：内径 0.1 mm、長さ 25 cm
達成値：内径 0.1 mm、長さ 35 cm、
伝送損失 3 dB 程度 (波長 1μm、長さ 20 cm)
と目標値を達成することが出来た。ファイバのバンドル化(280 本×2 個)により、銀鏡反応の際の流量 14.5 ml/min を実現し、良好な銀中空ファイバを製作できた。本研究で表面粗さの少ない良好な超細径銀中空ファイバが製作できたことにより、歯科内視鏡用内径 0.1 mm 無機薄膜内装銀中空ファイバの製作が期待できる。

平成21年度は無機ガラス薄膜内装中空ファイバの製作として、内径 0.1 mm、長さ 10cm、Er:YAG レーザ光の透過率 60%を目標とする。

E．健康危険情報

特になし

F．研究発表

1．論文発表

1) K. R. Sui, X. S. Zhu, X. L. Tang, K. Iwai, M. Miyagi, and Y. W. Shi, "Method for evaluating material dispersion of dielectric film in the hollow fiber," Appl. Opt. Vol. 47, No. 34, pp.6340-6344 (Dec. 2008)
2) T. Watanabe, K. Iwai, and Y. Matsuura, "Dual-wavelength laser irradiation through hollow optical fiber for hard tissue ablation," Proc. SPIE Vol. 6852, pp. 68520E-1-68520E-6 (2008).
3) M. Nemec, H. Jelinkova, M. Miyagi, K. Iwai, Y. W. Shi, Y. Matsuura, "Thin hollow glass waveguide for near IR radiation delivery," Proc. SPIE Vol. 6852, pp. 68520W-1-68520W-6 (2008).
4) K. Iwai, Y. W. Shi, M. Miyagi, X. S. Zhu, Y. Matsuura, "Fabrication of 100-μm-bore hollow fiber for infrared transmission," Proc. SPIE Vol. 6852, pp. 68520S-1-68520S-8 (2008).

2．国際学会発表

1) K. Iwai, M. Miyagi, Y. W. Shi, X. S. Zhu, and Y. Matsuura, "Fabrication of hollow optical fiber with a vitreous film for CO2 laser light delivery, " SPIE Photonics West 2009 Optical Fibers and Sensors for Medical Diagnostics and Treatment Applications IX, 7173-24, (Jan. 25, 2009).
2) T. Watanabe, K. Iwai, and Y. Matsuura, "Simultaneous radiation of Er:YAG and Ho:YAG lasers for efficient ablation of hard tissues," SPIE Photonics West 2009 Optical Fibers and Sensors for Medical Diagnostics and Treatment Applications IX, 7173-25, (Jan. 25, 2009).
3) K. R. Sui, X. Lin, X. S. Zhu, Y. W. Shi, K. Iwai, and M. Miyagi, "Fabrication of SiO_2/AgI/SiO_2/Ag hollow glass fiber for

infrared transmission," SPIE Photonics West 2009 Optical Fibers and Sensors for Medical Diagnostics and Treatment Applications IX, 7173-14, (Jan. 26, 2009).

4) M. Nemec, H. Jelinkova, M. Miyagi, K. Iwai, and Y. Matsuura, "250 μm inner diameter hollow waveguide for Er:YAG laser radiation," SPIE Photonics West 2009 Optical Fibers and Sensors for Medical Diagnostics and Treatment Applications IX, 7173-15, (Jan. 24, 2009).

5) T. Dostalova, H. Jelonkova, P. Koranda, J. Sulc, M. Nemec, M. Miyagi, and K. Iwai, "Laser brackets deponding: Tm:YAP, Nd:YAG, and two diode lasers evaluation," SPIE Photonics West 2009 Lasers in Dentistry XV, 7162-20, (Jan. 24, 2009).

3. 国内学会発表

1) 岩井 克全, 渡邊智紀, 松浦 祐司, "赤外レーザ光同時照射による軟組織の蒸散・凝固効果," 平成 20 年度電気関係学会東北支部連合大会講演論文集, 2E08, p. 177 (Aug. 22, 2008).

2) 岩井 克全, 宮城 光信, 石山 純一, "ポリエチレン内装銀中空ファイバの試作," 平成20年度電気関係学会東北支部連合大会講演論文集, 2E09, p. 178 (Aug. 22, 2008).

3) 岩井 克全, 宮城 光信, 石 芸尉, 松浦 祐司, "赤外レーザ用内径 100 μm 中空ファイバの製作," 電子情報通信学会通信ソサイエティ大会講演論文集, B-13-24, p. 278 (Sep. 17, 2008).

4) 渡邊 智紀, 岩井 克全, 松浦 祐司, "Er:YAG, Ho:YAG レーザの同時照射による硬組織の高効率蒸散," 電子情報通信学会通信ソサイエティ大会講演論文集, B-13-26, p. 280(Sep. 17, 2008).

5) 岩井 克全, 宮城 光信, 石 芸尉, 朱 暁松, 松浦 祐司, "CO_2 レーザー光伝送用無機薄膜内装中空ファイバの製作," 第 29 回レーザー学会学術講演会講演予稿集, , I312aIII06, p. 220 (Jan. 12, 2009).

6) 岩井 克全, 板垣 静香, 安藤 美帆, 宮城 光信, 石 芸尉, 松浦 祐司, "赤外伝送用超細径銀中空ファイバの製作,"電子情報通信学会総合大会講演論文集, B-13-2, p. 490 (Mar. 16, 2009).

G. 知的財産権の出願・登録状況

1. 特許取得
   特になし
2. 実用新案登録
   特になし
3. その他
   特になし

H. その他

1. 受賞

1) 2008 年 10 月 24 日, "超細径内視鏡用高機能中空ファイバの研究," 財団法人 石田記念財団 平成 20 年度石田記念財団研究奨励賞.

研究成果の刊行に関する一覧表

雑誌

発表者氏名	論文タイトル名	発表誌名	巻号	ページ	出版年
K. R. Sui, X. S. Zhu, X. L. Tang, K. Iwai, M. Miyagi, and Y. W. Shi	Method for evaluating material dispersion of dielectric film in the hollow fiber	Appl. Opt.	Vol. 47, No. 34	6340-6344	2008
T. Watanabe, K. Iwai, and Y. Matsuura	Dual-wavelength laser irradiation through hollow optical fiber for hard tissue ablation	Proc. SPIE	Vol. 6852	68520E-1-68520E-6	2008
M. Nemec, H. Jelinkova, M. Miyagi, K. Iwai, Y. W. Shi, Y. Matsuura	Thin hollow glass waveguide for near IR radiation delivery	Proc. SPIE	Vol. 6852	68520W-1-68520W-6	2008
K. Iwai, Y. W. Shi, M. Miyagi, X. S. Zhu, Y. Matsuura	Fabrication of 100-μm-bore hollow fiber for infrared transmission	Proc. SPIE	Vol. 6852	68520S-1-68520S-8	2008

国内学会予稿集

発表者氏名	論文タイトル名	発表誌名	巻号	ページ	出版年
岩井 克全, 渡邊 智紀, 松浦 祐司	赤外レーザ光同時照射による軟組織の蒸散・凝固効果	平成20年度電気関係学会東北支部連合大会講演論文集		177	2008
岩井 克全, 宮城 光信, 石 芸尉, 松浦 祐司	赤外レーザ用内径100μm中空ファイバの製作	電子情報通信学会通信ソサイエティ大会講演論文集		278	2008
渡邊 智紀, 岩井 克全, 松浦 祐司	Er:YAG, Ho:YAGレーザの同時照射による硬組織の高効率蒸散	電子情報通信学会通信ソサイエティ大会講演論文集		280	2008
岩井 克全, 宮城 光信, 石 芸尉, 朱 暁松, 松浦 祐司	CO_2レーザー光伝送用無機薄膜内装中空ファイバの製作	第29回レーザー学会学術講演会講演予稿集		220	2009

岩井 克全, 板垣 静香, 安藤 美帆, 宮城 光信, 石芸尉, 松浦 祐司	赤外伝送用超細径銀中空ファイバの製作	電子情報通信学会総合大会講演論文集		490	2009

Method for evaluating material dispersion of dielectric film in the hollow fiber

Ke-Rong Sui,[1] Xiao-Song Zhu,[1,*] Xiao-Li Tang,[1] Katsumasa Iwai,[2] Mitsunobu Miyagi,[2,3] and Yi-Wei Shi[1]

[1]Department of Communication Science and Engineering, Fudan University, Shanghai 200433, China

[2]Sendai National College of Technology, Sendai, 989-3128, Japan

[3]Miyagi National College of Technology, Sendai, 981-1239, Japan

*Corresponding author: zhuxiaosong@fudan.edu.cn

Received 14 July 2008; revised 17 September 2008; accepted 24 October 2008; posted 31 October 2008 (Doc. ID 98810); published 21 November 2008

A method is proposed to evaluate the material dispersion of dielectric film in dielectric-coated silver hollow fiber. Cauchy's formulas that characterize the dispersion property were obtained for several commonly used dielectric materials by using the measured data of loss spectra of the hollow fibers. The wavelengths of the loss peaks and valleys in the loss spectra can be predicted more accurately when taking into consideration of the material dispersion. The derived Cauchy's formulas play an important role in the design of infrared hollow fiber for multiwavelength delivery. © 2008 Optical Society of America

OCIS codes: 060.2280, 230.7370, 310.6860, 260.2030.

1. Introduction

Dielectric-coated silver hollow fiber is one of the most commonly used infrared fibers in many applications [1–4]. It has low-loss property in the mid-infrared region, as well as in the visible and near-infrared (VIS-NIR) regions [5,6]. For a hollow fiber with a uniform and smooth dielectric inner-coating film, there are high-loss peaks and low-loss valleys in the loss spectra for the hollow fiber due to thin film interference. It is possible to use these low-loss valleys for multiwavelength delivery of infrared lasers and visible pilot beams. In the design and fabrication of high-performance hollow fiber, the low-loss valleys should be accurately located at the target wavelengths. By adjusting the film thickness of the dielectric layer, we can shift the wavelength of the low-loss valley to match the objective wavelength. However, theoretical calculation results do not agree well with the measured loss spectra because of the material dispersion of the dielectric film, especially in the VIS-NIR regions. Although optical constants for some of the dielectric materials can be found in the literature or published handbooks [7,8], they do not have data in the VIS-NIR regions or do not agree with the dispersion property of the dielectric film in the hollow fiber. This is because the film in the hollow fiber is formed by using unique fabrication techniques [9,10].

In this paper, we proposed a method to evaluate the dispersion property by using measured loss spectra of hollow fibers with various film thicknesses. Cauchy's formulas [11] for several commonly used materials were obtained. By taking into consideration the material dispersion, the wavelengths of the low-loss valleys in the VIS-NIR regions can be predicted more accurately. The derived Cauchy's formulas are of special importance to the design of high-performance infrared hollow fiber for multiwavelength laser light delivery.

2. Sample Preparation

Loss spectra of hollow fiber with various dielectric film thicknesses were needed in the evaluation for material dispersion. To prepare the samples, we used

0003-6935/08/346340-05$15.00/0

the chemical deposition method [6] to plate the silver layer on the inner surface of a glass capillary. Then the dielectric layer was coated upon the silver layer. The liquid-phase coating method was used for many dielectric materials, such as polymers [6,12] and silicone polymer [13]. Dielectric layers with different film thickness could be formed by modifying the concentration of the coating solution or the flowing speed in the fabrication process. For silver iodide (AgI) film, the iodination process [5] was used to turn the upper-side silver into AgI. The thickness of the AgI film could be controlled by changing iodination time, iodination temperature, or concentration of the iodination solution. For all of the hollow fiber samples made for the evaluation, the bore diameter is 0.7 mm and the length is around 25 cm.

3. Theoretical Evaluation

The loss spectrum of the dielectric-coated metallic hollow fiber has been theoretically evaluated [14,15]. For a hollow fiber of length z, the transmitted power $P(z)$ is

$$P(z) = \int_0^{\theta_{\max}} P_0(\theta) \exp\left[-\frac{1-R(\theta)}{2T\cot\theta} z\right] \sin\theta \mathrm{d}\theta, \qquad (1)$$

where $P_0(\theta)$ is the angular distribution of the incident beam, $R(\theta)$ is the power reflection coefficient, T is the inner radius of the hollow core, and $\theta_{\max}$ denotes the maximum launching angle. Theoretical result of loss spectrum for the hollow fiber was obtained by calculating $P(z)$ in a certain wavelength region. Because the power reflection coefficient $R(\theta)$ is dependent on the refractive index of the dielectric film, material dispersion has a great influence on the position of low-loss valleys in the loss spectra.

There are normally obvious interference peaks in the measured loss spectra of the hollow fiber when a uniform and smooth inner dielectric film is formed. These peaks at various wavelengths, along with the film thickness, contain information on the dispersion property of the dielectric film. We use Cauchy's formula $n(\lambda) = A + B/\lambda^2 + C/\lambda^4$ [11] to evaluate the dispersion. In order to calculate the constants A, B, and C in Cauchy's formula, we need the measured loss spectra of the hollow fiber with different film thicknesses. Loss spectra in the VIS-NIR regions were measured for samples prepared as described in Section 2. Figure 1 is the schematic setup for measuring the loss spectrum of the hollow fiber in the VIS-NIR regions. An incoherent white light was used as the light source, and it was coupled into the hollow fiber through a GI fiber with 600 μm core diameter. The light at the output end was received by the spectrum analyzer (Advantest Q8344A). Loss spectra of the hollow fiber were obtained by comparing the output light with the input light as the background.

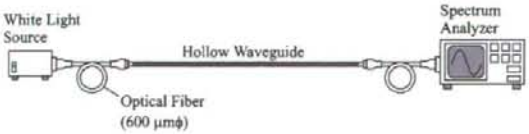

Fig. 1. Schematic setup for loss spectrum measurement.

Due to the difference of film thicknesses among samples, loss peaks, and valleys appeared at various wavelengths in their loss spectra. For each loss spectrum, we define λ_m as the mth wavelength from longer to shorter wavelength at which loss peak appears. Also, $n_i(\lambda_m)$ is defined as the refractive index at the wavelength of λ_m in the ith loss spectrum. The order of the loss spectra was arranged randomly. Here we take AgI material as an example to show the evaluation method for Cauchy's formula in VIS-NIR regions.

1. $n_1(\lambda_1)$, the refractive index of AgI at the wavelength of λ_1 in the first loss spectrum, is taken from the literature [8] as the initial value in the calculation circles.
2. Make λ_1 in the theoretical loss spectrum agree with the λ_1 in the measured loss spectrum by adjusting the film thickness, and we get a film thickness d.
3. By using the thickness d in step (2), make λ_2 in the theoretical loss spectrum agree with the λ_2 in the measured loss spectrum by adjusting the refractive index at the wavelength λ_2. Then we get $n_1(\lambda_2)$.
4. Do step (3) to other $\lambda_m(\lambda_3, \lambda_4 \ldots)$, and we get the refractive indices of AgI at the wavelengths of all the peaks in this measured loss spectrum, $n_1(\lambda_m)$.
5. Repeat steps (1) to (4) for all the measured loss spectra. Record the data of $n_i(\lambda_m)$ of every loss spectrum and put them together, then we get a group of refractive index–wavelength data $n_i(\lambda_m)$ for the AgI material ($i = 1, 2, 3, \ldots$, $m = 1, 2, 3, \ldots$).
6. Use Cauchy's formula $n(\lambda) = A + B/\lambda^2 + C/\lambda^4$ as the formula to fit the data of refractive indices in step (5), and we get an empirical formula of material dispersion for the AgI film.
7. New $n_i(\lambda_m)$ are calculated by the empirical formula for every measured loss spectrum and it is used in step (1) in the next calculation cycle instead of the initial one.
8. Repeat steps (1) to (7) and new formulas are gotten in every cycle. Stop the process when the difference between film thicknesses d in two continuous circles is smaller than 1% for all the measured loss spectra.

Finally, an empirical formula of material dispersion for the AgI film in the AgI/Ag hollow fiber is derived.

As a consequence of the fabrication techniques [16], the thickness of the dielectric film can be tapered along the length of fiber. The tapered thickness will widen the interference peaks in the loss spectra and the position of the peaks should be determined by the average thickness. The thickness d in the evaluation method refers to the average thickness of the dielectric film, and therefore the slightly tapered film does not affect the evaluation method. Moreover,

because the fiber samples fabricated for the evaluation were of short length, we can neglect the variation of film thickness along the fiber.

4. Results

We have applied this method to four kinds of commonly used dielectric materials in the hollow fiber. They are cyclic olefin polymer (COP) [6], silicone polymer (R_2SiO) [12], Arton polymer [13], and AgI [5]. The empirical formulas of their dispersion properties have been calculated. The constants A, B, and C in the empirical formula for the four kinds of material are summarized in Table 1, where λ is in micrometers. In our recent paper [17], the empirical formula of AgI proved that it is helpful for accurately predicting the transmission properties of the hollow fiber in the VIS-NIR regions.

Figure 2 shows the refractive indices of AgI and R_2SiO in the VIS-NIR regions. Curves 1 and 3 (dashed lines with data dots) are data of AgI and silicon dioxide (SiO_2) in the literature [8]. Curves 2 and 4 (solid lines) are results obtained by using the empirical formula in Section 3. Normally, the optical constants in the literature were obtained by measuring the optical properties of bulk material. Thin film has different optical properties from that of the bulk material. This is because bulk material and thin film are made by using different fabrication processes, and the crystalline phase of the material may not be the same, e.g., AgI [18]. Moreover, the R_2SiO film formed by using silicone polymer was a vitreous layer that was similar to but not pure SiO_2. This might be the reason for the large difference between curves 3 and 4. Figure 3 shows the refractive indices of COP and Arton calculated by the empirical formula. We have not found any other dispersion data about COP and Arton for comparison.

It can be seen in Figs. 2 and 3 that the refractive indices of the four kinds of material change more rapidly in the visible region. Therefore in the loss spectra of the hollow fiber, the intervals between adjacent peaks in visible region are much smaller than that in the infrared region. We should pay more attention to the dispersion property of the dielectric film in the VIS-NIR regions when designing an infrared hollow fiber for simultaneous delivery of a visible laser light. In addition, if the dielectric material has no resonance absorptions in the mid-infrared region, this method can also be applied to the evaluation for the dispersion property of the dielectric film in the mid-infrared regions.

Table 1. Constants in Cauchy's formula for Four Kinds of Dielectric Film Materials in Hollow Fiber

Material	A	B	C
COP	1.50815	0.01653	−0.00026
R_2SiO	1.42614	0.02729	0.0001
Arton	1. 52743	0.01855	0.00028
AgI	2.0216	0.0878	−0.0024

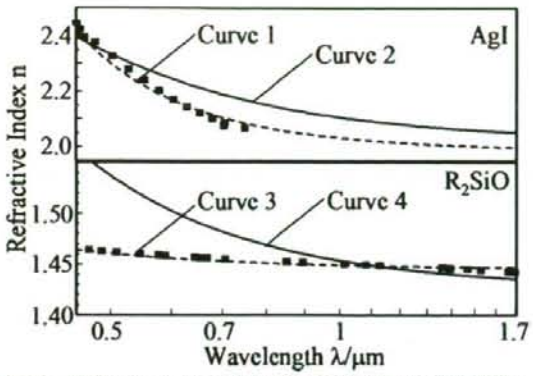

Fig. 2. Refractive indices of AgI and R_2SiO in the VIS-NIR regions. The dashed lines with data dots are from the data published in the literature [8].

Figure 4 is the loss spectra of the R_2SiO-coated silver (R_2SiO/Ag) hollow fiber. The fiber was of 0.7 mm bore size and 1 m length. Calculated 1 corresponds to the theoretical result considering material dispersion from the empirical formula (i.e., curve 4 in Fig. 2). Calculated 2 corresponds to the result considering material dispersion from the literature [8] (i.e., curve 3 in Fig. 2), and calculated 3 corresponds to the result without considering material dispersion. It can be seen that calculated 1 agrees well with the measured result. Calculated 2 and 3 did not agree with the measured result especially in the visible wavelength region. The disagreement may cause mistakes in structure design for the hollow fiber. That is, the loss valley will be arranged at the wrong wavelength when we neglect the material dispersion or take inappropriate data about the material dispersion.

Figure 5 shows the measured loss spectra of R_2SiO/Ag, Arton-coated silver (Arton/Ag), COP-coated silver (COP/Ag), and AgI/Ag hollow fibers. Fibers are 1 m long and 0.7 mm in diameter. None of these measured spectra was used in the calculation

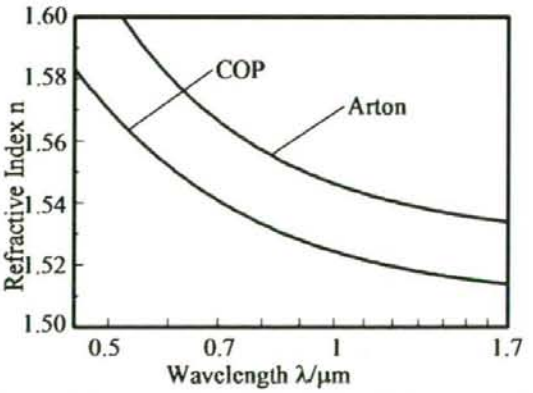

Fig. 3. Refractive indices of COP and Arton polymer in the VIS-NIR regions.

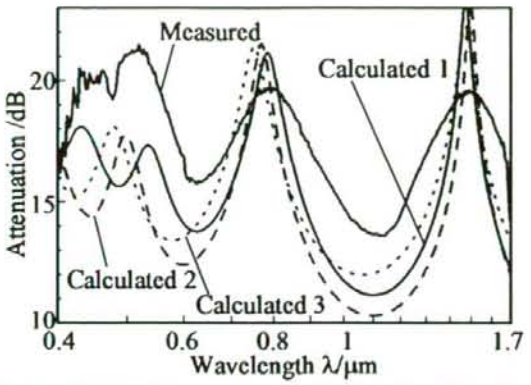

Fig. 4. Theoretical loss spectra of R_2SiO/Ag hollow fiber calculated by using different material dispersion formulas. Measured loss spectrum is also shown for comparison.

in Section 3 for deriving Cauchy's formula. Theoretical loss spectra considering material dispersion from the empirical formulas are also included. In the calculation the absorption of material was neglected, because the absorption in the VIS-NIR regions is very small, normally smaller than 10^{-3} [19]. There is a discrepancy in loss values between measurements and calculations in Fig. 5. Absorption of the material is one reason for the discrepancy. Another reason is the nonuniformity of the dielectric film thickness, which causes additional loss. Moreover, the surface roughness was set to be a certain value in the calculation. This may also cause a discrepancy in the loss magnitude. The results in this paper are qualitatively rather than quantitatively correct, which is due to the approximate nature of the Cauchy's formula and the above-mentioned reasons. But the formula is supposed to be used for predicting the positions of loss valleys, which are most important in the structure design for high-performance hollow fibers. And good agreement between valley positions shows that it works rather well when taking into consideration the derived dispersion. That is, the derived Cauchy's formula characterized the dispersion property of the dielectric film in the hollow fiber well.

5. Conclusions

Material dispersion plays an important role in the design of high-performance dielectric-coated metal hollow fiber. For most of the commonly used dielectric film materials in the hollow fiber, there are few data about the dispersion property in the VIS-NIR regions. And some data found in handbooks do not agree with the dispersion property of the film due to different fabrication techniques. We proposed a method to evaluate the material dispersion of the dielectric film in the hollow fiber. Empirical formulas for four kinds of dielectric film materials were derived according to Cauchy's formula of material

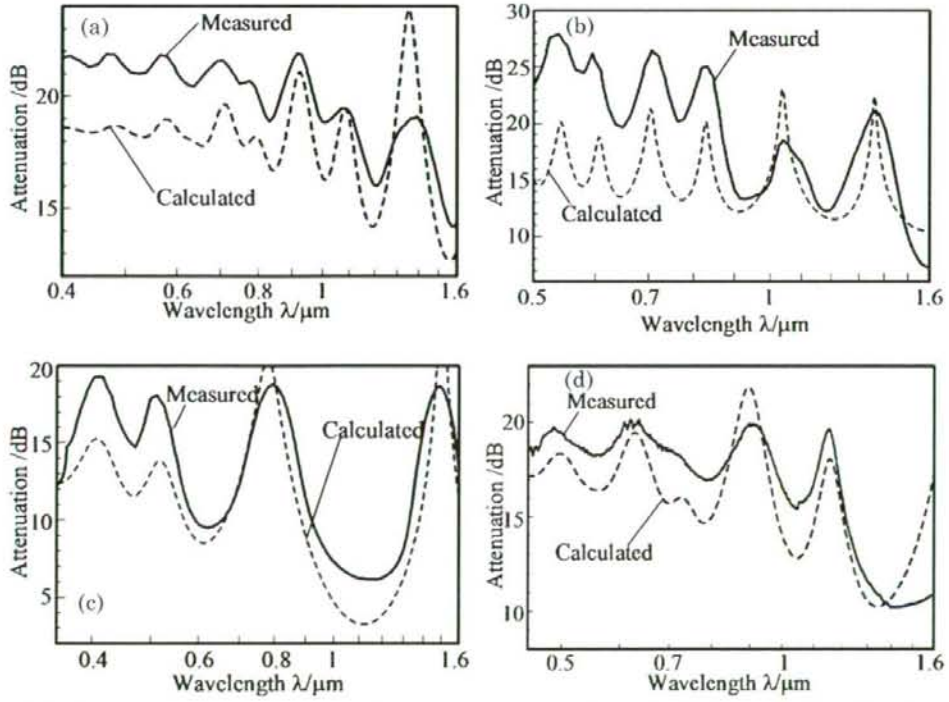

Fig. 5. Theoretical and measured loss spectra of the dielectric-coated silver hollow fibers. (a) R_2SiO, (b) Arton/Ag, (c) COP/Ag, and (d) AgI/Ag hollow fiber.

dispersion. By taking into consideration of the material dispersion with these formulas, the wavelengths of the low-loss valleys in the VIS-NIR regions can be predicted more accurately in the structure design for the hollow fiber. These formulas provide an important role for the design of high performance dielectric-coated silver hollow fiber. The basic thought of this method may also be helpful in other optical experiments for deriving optical constants from experimental measured data.

This work is financially supported by the National Nature Science Foundation of China (NSFC, 60608013), the Shanghai Pujiang program (7pj14012), and the Ministry of Education, Science, Sports and Culture of Japanthrough Grant-in-Aids for Scientific Research (B) (20360164).

References

1. V. Gopal, J. A. Harrington, A. Goren, and I. Gannot, "Coherent hollow-core waveguide bundles for infrared imaging," Opt. Eng. **43**, 1195–1199 (2004).
2. S. Sato, Y. W. Shi, Y. Matsuura, M. Miyagi, and H. Ashida, "Hollow-waveguide-based nanosecond, near-infrared pulsed laser ablation of tissue," Lasers Surg. Med. **37**, 149–154 (2005).
3. J. Raif, M. Valid, O. Nahlieli, and I. Gannot, "An Er:YAG laser endoscopic fiber delivery system for lithotripsy of salivary stones," Lasers Surg. Med. **38**, 580–587 (2006).
4. H. Jelinkova, T. Dostalova, M. Nemec, P. Koranda, M. Miyagi, K. Iwai, Y. W. Shi, and Y. Matsuura, "Free-running and Q-switched Er:YAG laser dental cavity and composite resin restoration," Laser Phys. Lett. **4**, 835–839 (2007).
5. R. George and J. A. Harrington, "Infrared transmissive, hollow plastic waveguides with inner Ag-AgI coatings," Appl. Opt. **44**, 6449–6455 (2005).
6. Y. W. Shi, K. Ito, L. Ma, T. Yoshida, Y. Matsuura, and M. Miyagi, "Fabrication of a polymer-coated silver hollow optical fiber with high performance," Appl. Opt. **45**, 6736–6740 (2006).
7. Y. Wang, Y. Abe, Y. Matsuura, M. Miyagi, and H. Uyama, "Refractive indices and extinction coefficients of polymers for the mid-infrared region," Appl. Opt. **37**, 7091–7095 (1998).
8. E. D. Palik, *Handbook of Optical Constants of Solids* (Academic, 1985).
9. Y. Matsuura, T. Abel, and J. A. Harrington, "Optical properties of small-bore hollow glass waveguides," Appl. Opt. **34**, 6842–6847 (1995).
10. Y. Kato, M. Osawa, M. Miyagi, M. Aizawa, S. Abe, and S. Onodera, "New fabrication technique of fluorocarbon polymer-coated hollow waveguides by liquid-phase coating for medical applications," Proc. SPIE **2131**, 4–10 (1994).
11. M. Born and E. Wolf, *Principles of Optics*, 7th ed. (Cambridge U. Press, 1999).
12. S. Ouyang, Y. W. Shi, Y. Matsuura, and M. Miyagi, "Rugged distal tips for CO_2 laser medicine," Opt. Laser Technol. **35**, 65–68 (2003).
13. K. Iwai, M. Miyagi, Y. W. Shi, X. S. Zhu, and Y. Matsuura, "Infrared hollow fiber with a vitreous film as the dielectric inner coating layer," Opt. Lett. **32**, 3420–3422 (2007).
14. Y. Matsuura, M. Saito, M. Miyagi, and A. Hongo, "Loss characteristics of circular hollow waveguides for incoherent infrared light," J. Opt. Soc. Am. A **6**, 423–427 (1989).
15. M. Miyagi and S. Kawakami, "Design theory of dielectric-coated circular metallic waveguides for infrared transmission," J. Lightwave Technol. **2**, 116–126 (1984).
16. K. Iwai, Y. W. Shi, M. Miyagi, and Y. Matsuura, "Improved coating method for uniform polymer layer in infrared hollow fiber," Opt. Laser Technol. **39**, 1528–1531 (2007).
17. K. R. Sui, Y. W. Shi, X. L. Tang, X. S. Zhu, K. Iwai, and M. Miyagi, "Optical properties of AgI/Ag hollow fiber in the visible wavelength region," Opt. Lett. **33**, 318–320 (2008).
18. R. Dahan, J. Dror, and N. Croitoru, "Characterization of chemically formed silver iodide layers for hollow infrared guides," Mater. Res. Bull. **27**, 761–766 (1992).
19. Y. Wang and M. Miyagi, "Simultaneous measurement of optical constants of dispersive material at visible and infrared wavelengths," Appl. Opt. **36**, 877–884 (1997).

Dual-wavelength laser irradiation through hollow optical fiber for hard tissue ablation

Tomonori WATANABE [1], Katsumasa IWAI [2], and Yuji MATSUURA [1]

1) Tohoku University, Department of Electrical Communications, Sendai 980-8579, Japan
2) Sendai National College of Technology, Sendai 989-3128, Japan

Abstract

Laser ablation experiments on hard tissues are performed by guiding combined beam of Ho:YAG and Er:YAG laser light with a hollow optical fiber. An alumina ball is used as a hard-tissue model and ablation phenomenon are observed by an ultra-high-speed camera. The result show that the two laser light give dissimilar ablation effects due to different absorption coefficients in water contained in the tissues. When the two lasers are combined and irradiate on the model, a high ablation rate is observed.

Keywords: Laser treatment, Hard tissue ablation, Infrared lasers, Hollow optical fibers

1. Introduction

Since bio-tissues contains water that strongly absorbs infrared light, irradiation by infrared light has a large effect on both of hard and soft tissues and therefore, it is applied to variety of medical applications[1]. Low invasive therapies using a laser endoscope have been developed to radiate laser light inside human body by using an optical fiber incorporated in the endoscope. These laser endoscopes are getting popular in urological applications such as ablation of the prostate and fragmentation of urinary calculi and usually, Nd:YAG lasers with the wavelength of 1.06 μm or Ho:YAG lasers of 2.1 μm is used because a common silica-glass fiberoptics can be employed as delivery medium of laser light[2]. Recently an Er:YAG laser with the 2.94-μm wavelength is reportedly more effective for calculus fragmentation[3] because the laser light is strongly absorbed with calcium oxalate and magnesium ammonium phosphate contained in urinary calculi[4].

Er:YAG lasers have, however, a drawback that a flexible silica-glass fiber cannot be used for laser delivery because of the absorption losses at the relatively long wavelength of 2.94 μm. Our group have proposed and developed a hollow optical fiber for Er:YAG laser delivery. Hollow optical fibers have no absorption loss in the airy core and show highly efficient transmission for any wavelengths in the infrared. Because the hollow optical fibers also have high durability for laser radiation, they are already employed as a flexible transmission line in laser treatment systems in the market.

Optical Fibers and Sensors for Medical Diagnostics and Treatment Applications VIII,
edited by Israel Gannot, Proc. of SPIE Vol. 6852, 68520E, (2008) · 1605-7422/08/$18
doi: 10.1117/12.761421

In this paper, we investigate effects of simultaneous irradiation by Ho:YAG and Er:YAG lasers on hard tissues such as calculi and teeth. Although there have been some reports on irradiation of lasers with different wavelengths for medical applications, they usually are for incision and ablation of soft tissues where both of high incision rate and hemostatic effect are required[5]. Here we investigate ablation mechanisms of the lasers to achieve higher ablation effect for hard tissues.

2. Experiment and Discussion

We used an experimental setup shown in Fig. 1 to irradiate a hard tissue model with the two different lasers light. Ho:YAG and Er:YAG laser light are combined by using a dichroic mirror and the laser beam is focused by a f=76 mm CaF_2 lens on the input end of a short hollow-fiber tip (100 mm in length) employed as a coupling optics. A hollow optical fiber with an inner diameter of 0.7 mm is butt-coupled to the short fiber that has the same diameter. The hollow fiber is coated with silver and cyclic-olefin polymer (COP) thin film on the inside[6] and the thickness of COP is 0.3 μm so that the transmission losses for both of Er:YAG and Ho:YAG lasers are reduced by interference effect of the polymer film that acts as a reflection enhancement coating. The transmission losses of the hollow optical fiber used in the experiment are 1.0 dB for Ho:YAG and 0.5 dB for Er:YAG laser light.

The distal end of the hollow optical fiber is capped to keep the inside of fiber from vapor and debris of the ablated tissues. We proposed, for hollow optical fibers, glass lens caps that offer a high ablation efficiency owing the higher energy intensity of focused beam[7]. In the experiment, we used two kinds of caps that are, as shown in Fig. 2, a ball-lens cap and a hemispherical lens cap. The focusing effect of the caps is shown in Fig. 3 as changes of measured beam sizes in distance from the lens surface. The result show that focal lengths of the caps are 1.0 mm for the hemispherical and 0.1 mm for the ball lens caps. The insertion loss of the cap is around 15% and therefore, the energy density at the focused spot is around twice of the unfocused beam.

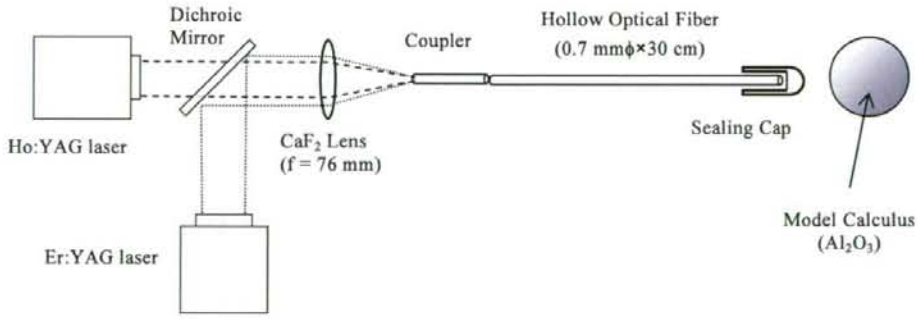

Fig. 1 Experiment setup for dual-wavelength irradiation

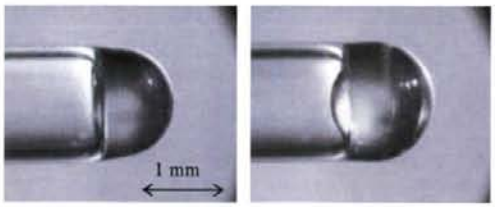

(a) Hemisphere (b) Ball

Fig. 2 Focusing glass caps for hollow optical fibers

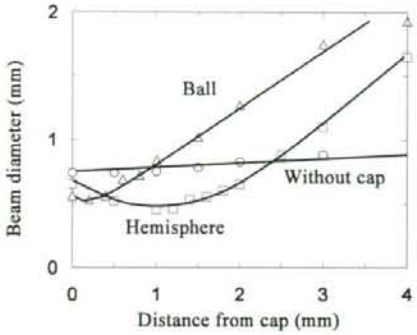

Fig. 3 Beam diameter in distance from cap surface

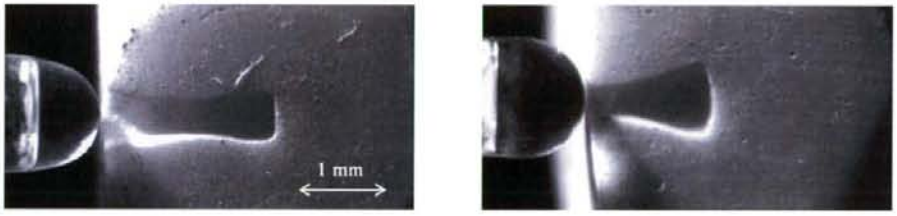

(a) Using hemisphere cap (b) Using ball lens cap

Fig. 4 Cutting sections of ceramic balls after irradiated with Er:YAG laser pulses

To test the ablation capability of the lens caps, Er:YAG laser light irradiates alumina ceramic balls used as a hard tissue model. The balls are 4-7 mm in diameter and immersed in water before the test so that the balls contain water in high volume. Figure 4 shows cutting sections of the balls after irradiated with 10 Er:YAG-laser pulses of 300 μs in pulse width, 10 Hz in frequency, and 100 mJ in pulse energy. The result shows that ablation depth is around 40% larger in the one employed the hemisphere cap and this is because of the smaller divergence angle from the cap. From this result, we used the hemisphere cap in the experiments hereafter.

We firstly compared ablation capabilities of Ho:YAG and Er:YAG laser light for hard tissues by evaluation of depth and width of ablated holes as a function of number of laser pulses. Pulse energy used in the test was 100 mJ at repetition rate of 10 Hz and the pulse widths are 250 μs for Ho:YAG and 300 μs for Er:YAG lasers. As seen from the result in Fig. 5, the widths are comparable for the both lasers and, in contrast, the result on the depth shows different appearances for the two lasers. When irradiated with Er:YAG laser light, the depth linearly increases with the number of pulses. For the Ho:YAG, however, it is saturated with number of pulses. This is because energy density of the laser beam falls the ablation threshold of hard tissues when the beam

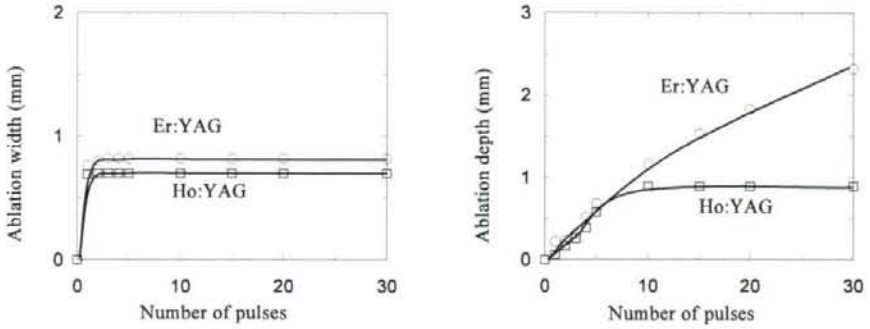

Fig. 5 Depth and width of ablated holes as a function of number of laser pulses

spreads due to focusing effect of the lens cap. This happens in lower energy density for the Ho:YAG laser because of the lower absorption coefficient in water.

Secondly we observed ablation phenomenon by using an ultra-high-speed camera to investigate difference in the ablation mechanisms of the two lasers. Figure 6 shows a moment of ablation with laser pulse energy of 100 mJ recorded at 50,000 frame/sec of capture speed. When irradiated with Er:YAG laser light, powdery dust are scattered from the surface immediately after laser radiation. This is because the laser energy is absorbed in very surface of the tissue. On the other hand, for the Ho:YAG laser, relatively large debris are spattered after the surface swelled. The laser beam penetrates into the tissue and an explosive ablation occurred from the inside. From these results, we expect, owing to the different ablation mechanisms, a high ablation effect when properly combining the two lasers beams.

In the next experiment, the two laser beams are combined and shoot an alumina ball to investigate effects of simultaneous irradiation. The pulse energies are 200 mJ for Ho:YAG and 100 mJ for Er:YAG laser,

(a) Er:YAG (b) Ho:YAG

Fig. 6 Moment of ablation with Er:YAG and Ho:YAG laser pulse